Synthesis and Electrochromic Properties of Novel Aromatic Polyamides Bearing Ether-linked Bis(triphenylamine) Units

NSC 97-2221-E-027-113-MY3

Shou-Lun Cheng (鄭守倫), Hui-Min Wang (王惠民), Sheng-Huei Hsiao (蕭勝輝)*
Department of Chemical Engineering and Biotechnology, National Taipei University of Technology
(國立臺北科技大學化學工程與生物科技系)
Tel: +886-2-27712171 ext. 2548; Fax: +886-2-27317117
E-mail: shhsiao@ntut.edu.tw

Abstract

A new class of electroactive polyamides with ether-linked bis(triphenylamine) [O(TPA)$_2$] units were prepared *via* the direct phosphorylation polycondensation from {4-[di(4-aminophenyl)-amino]-4'-(diphenylamino)}diphenyl ether (**6**) and aromatic dicarboxylic acids. These polyamides were amorphous with good solubility in many organic solvents, such as *N*-methyl-2-pyrrolidinone (NMP) and *N*,*N*-dimethylacetamide (DMAc), and could be solution-cast into flexible polymer films. The polyamides exhibited good thermal stability with glass-transition temperatures in the range of 218-253 °C and 10% weight-loss temperatures in excess of 500 °C. Cyclic voltammograms of the polyamide films cast onto an indium-tin oxide (ITO)-coated glass substrate exhibited two reversible oxidation redox couples at 0.80~0.82 V and 0.96~0.98 V *versus* Ag/AgCl in acetonitrile solution. The polyamide films revealed excellent electrochemical and electrochromic stability, with a color change from a colorless or pale yellowish neutral form to green and purple oxidized forms at applied potentials ranging from 0 to 1.2 V.

1. Introduction

Electrochromic materials consist of redox-active species that exhibit significant, lasting, and reversible changes in color upon electrochemical reduction or oxidation.[1] Research in electrochromic devices has received a great deal of attention due to the importance of this interesting phenomenon in applications such as electrochromic windows, displays, memory devices, electronic papers, and adaptive camouflages. There is a vast amount of chemical species that exhibited electrochromic properties, including metal coordination complexes, metal oxide (especially tungsten oxide), viologens (4,4'-bipyridium salts), and conducting polymers (such as polyanilines, polypyrroles, and polythiophenes). The use of conjugated polymers as active layers in electrochromic devices became popular due to the advantageous properties such as fast switching time, ease of synthesis, and wide range of colors.[2] For efficient operation of an electrochromic device, it is necessary to take a number of properties into consideration: electrochromic efficiency, optical contrast, response time, stability and durability. The difficulty in achieving satisfactory values for all these parameters at the same time stimulates the development of new methods of preparation of electrochromic films, new materials and components for the devices.[3]

Triarylamine derivatives are well known for photo- and electroactive properties that may find optoelectronic applications as photoconductors, hole-transporters, and light-emitters.[4] Triarylamines can be easily oxidized to form stable radical cations, and the oxidation process is always associated with a noticeable change of coloration. Thus, many triarylamine-based electrochromic polymers have been reported in literature.[5] In recent years, Liou's and our groups have carried out extensive studies on the design and synthesis of triarylamine-based high-performance polymers such as aromatic polyamides and polyimides for potential electrochromic applications.[6] In general, these polymers exhibit good solubility to organic solvents due to the introduction of bulky, packing-disruptive triarylamine moieties. In addition, by incorporating the triarylamine units of different electronic nature into the polymer backbone, different oxidation levels of the polymers could be accessed, which make them to be a multi-electrochromic material. In a continuation of our recent efforts to explore high-performance electrochromic polymers, this work describes the synthesis of a new O(TPA)$_2$ containing diamine **6** and its derived electroactive aromatic polyamides. The structures of synthesized compounds and polymers were determined by FTIR and NMR spectroscopy. The optical, thermal, electrochemical, and electrochromic properties of the polyamides were investigated.

2. Monomer synthesis

The target aromatic diamine monomer, {4-[di(4-aminophenyl)-amino]-4'-(diphenylamino)}diphenyl ether (**6**), was synthesized starting from diphenylamine by a six-step reaction sequence as depicted in Scheme 1. In first step, the intermediate compound, 4-methoxytriphenylamine (**1**) was synthesized via Ullmann reaction between diphenylamine and 4-iodoanisole by using copper powder. Demethylation of compound **1** with boron tribromide gave the 4-hydroxytriphenylamine (**2**). Then, 4-nitropheoxytriphenyl-amine (**3**) was prepared by the nucleophilic aromatic fluoro-displacement reaction of *p*-fluoronitrobenzene with compound **2** in the presence of cesium fluoride (CsF). Reduction of the nitro group of compound **3** by means of hydrazine and Pd/C gave 4-aminophenoxytriphenylamine (**4**). The target diamine monomer **6** was prepared by hydrazine Pd/C-catalyzed reduction of dinitro compound **5**, resulting from the CsF-assisted *N*,*N*-diarylation reaction of compound **4** with two equivalent amount of *p*-fluoronitrobenzene.

The chemical structures of all the intermediate compounds and the target compound **6** were verified by NMR and FTIR spectra. Figure 1 illustrates the ^{1}H NMR and ^{13}C NMR spectra of the diamine monomer **6**. The assignments of all proton and carbon signals were assisted by the 2-D NMR spectra. These spectra are in good agreement with the proposed molecular structure of **6**. FTIR spectra of the synthesized compounds are also consistent with expected structures.

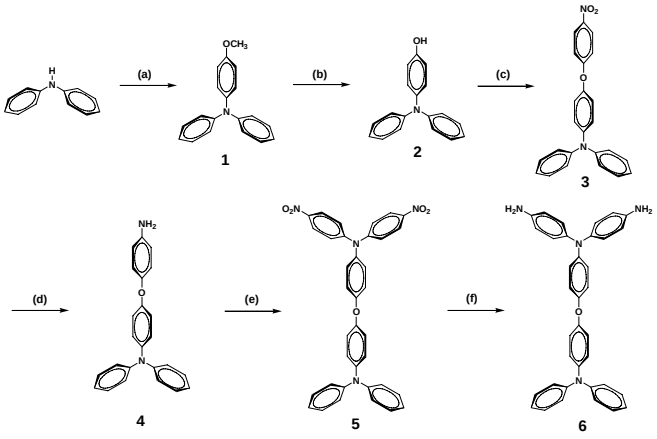

Scheme 1. Synthetic route to the target diamine monomer **6**. (a) 4-iodoanisole, Cu, K_2CO_3, TEGDME, 180 °C; (b) BBr_3, $CHCl_3$, rt, then MeOH; (c) *p*-fluoronitrobenzene, CsF, DMSO, 140 °C; (d) Pd/C, hydrazine, EtOH, reflux; (e) *p*-fluoronitrobenzene, CsF, DMSO, 140 °C; (f) Pd/C, hydrazine, EtOH, reflux.

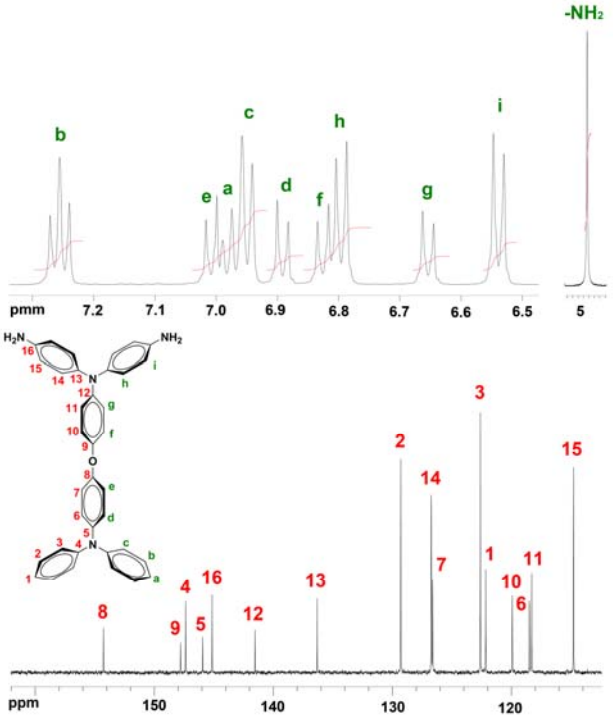

Figure 1. (a) ^{1}H NMR and (b) ^{13}C NMR spectra of diamine monomer **6** in DMSO-d_6.

3. Polymer synthesis

According to the phosphorylation polyamidation technique described by Yamazaki and coworkers,[7] a series of novel polyamides (**8a-8d**) with $O(TPA)_2$ units were synthesized from the diamine **6** and various aromatic dicarboxylic acids **7a-7d** using triphenyl phosphite (TPP) and pyridine as condensing agents (Scheme 2). The obtained polyamides had inherent viscosities in the range of 0.31~0.44 dL/g and could be solution-cast into flexible and tough films, indicating high molecular weight polymers.

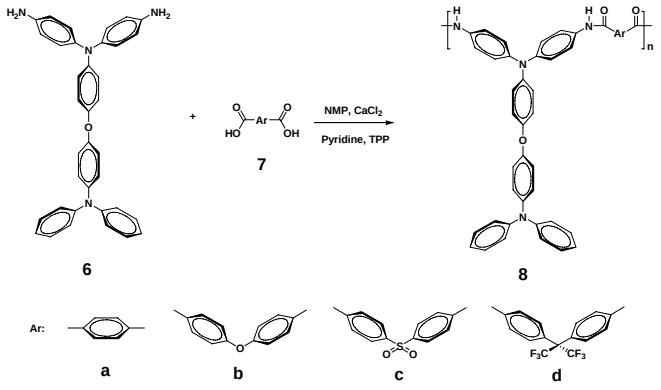

Scheme 2. Synthesis of polyamides **8a-8d**

4. Solubility and film property

The solubility behavior of polyamides was tested qualitatively, and the results are summarized in Table 1. All the polyamides were readily soluble in polar solvents such as NMP, DMAc, DMF, and DMSO, and the high solubility could be attributed to the introduction of the three-dimensional TPA moiety in the main chain and as a pendant group through ether linking. Thus, the excellent solubility makes these polymers potential candidates for practical applications by common solution processes to afford high performance thin films for optoelectronic devices. The polyamide **8d** also showed good solubility in less polar solvents like THF because of the additional contribution of the hexafluoroisopropylidene (-C(CF$_3$)$_2$-) fragment in the polymer backbone.

5. Thermal properties

The thermal properties of the polyamides were investigated by TGA and DSC techniques. The thermal behavior data are summarized in Table 1. Their decomposition temperatures (T_d) at a 10 % weight-loss in nitrogen and air were recorded at 556~568 and 537~555 °C, respectively. These polyamides left high carbonized residue (char yield) in excess of 65 % at 800 °C in an inert atmosphere, due to their high aromatic content. The glass-transition temperatures (T_g) of all the polyamides were observed in the range of 218-253 °C by DSC (Figure 2). All the polymers indicated no clear melting endotherms up to the decomposition temperatures on the DSC thermograms. The lowest T_g value (218 °C) associated with polyamide **8b** can be explained in terms of the flexible ether linkage in its diacid component. The thermal analysis results revealed that these polyamides exhibited good thermal stability, which in turn is beneficial to increase the service time in device application and enhance the morphological stability to the spin-coated film.

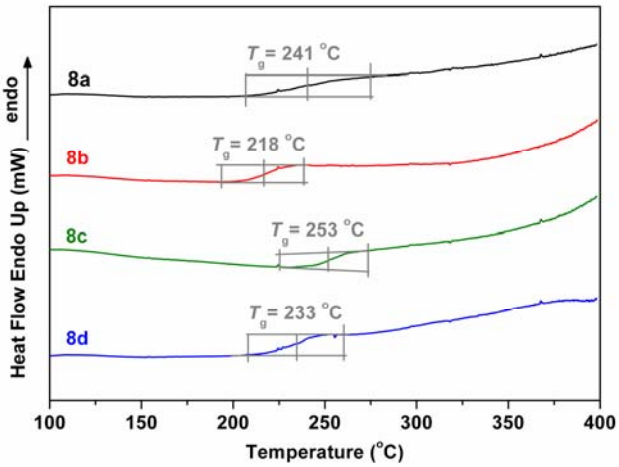

Figure 2. DSC curves of polyamides **8a-8d** with a heating rate of 20 °C/min.

Table 1 Inherent Viscosity, Solubility Behavior and Thermal Properties of the Polyamides

Polymer code	η_{inh}[a] (dL/g)	Solubility in various solvents[b]						T_g (°C)[c]	T_d at 10 wt% (°C)[d]		Char yield (wt %)[e]
		NMP	DMAc	DMF	DMSO	*m*-cresol	THF		In N_2	In air	
8a	0.44	++	++	++	++	+	–	241	565	555	76
8b	0.33	++	++	++	++	+–	+–	218	567	538	65
8c	0.38	++	++	++	++	+	+–	253	556	537	66
8d	0.31	++	++	++	++	+	++	233	568	545	69

[a] Measured at a polymer concentration of 0.5 g/dL in DMAc–5 wt % LiCl at 30 °C. [b] The qualitative solubility was tested with 10 mg of a sample in 1 mL of stirred solvent.. Notation: + +, soluble at room temperature; +, soluble on heating; +–,. partially soluble; –, insoluble even on heating. [c] Midpoint temperature of the baseline shift on the second DSC heating trace (rate = 20 °C/min) of the sample after quenching from 400 °C to 50 °C (rate = -200 °C/min) in nitrogen.. [d] Decomposition temperature, recorded *via* TGA at a heating rate of 20 °C/min and a gas-flow rate of 30 cm^3/min. [e] Residual weight percentage at 800 °C in nitrogen.

6. Electrochemical properties

The electrochemical behavior of the polyamides was investigated by cyclic voltammetry (CV) and pulse voltammetry (DPV) conducted for the cast film on an ITO-coated glass substrate as working electrode immersed in dry acetonitrile (CH_3CN) containing 0.1 M of Bu_4NClO_4 as an electrolyte under nitrogen atmosphere. In comparison to CV, DPV offers a higher sensitivity and sharper redox onsets throughout the electrochemical process owing to a reduced contribution of the charging background currents which, in turn, enhances the accuracy and reliability of the bandgaps estimated electrochemically. Figure 3 shows the CV and DPV curves for all polyamides, and the relevant oxidation potential data are summarized in Table 2. There are two reversible oxidation redox couples with half-wave potentials ($E_{1/2}$) of 0.80~0.82 V and 0.96~0.98 V at scan rate of 50 mV/s. During the CV scanning, we also found these polyamides showed interesting multi-colored electrochromic behaviors with coloration changing from colorless through green to purple. The CV curves for model compounds **M1**-**M3** are shown in Figure 4. When comparing the CV curves of **M3** and **M1**, we believe that the first oxidation peak appears to involve one electron loss from the main-chain TPA unit. This can be rationalized because this TPA segment is more electron-rich and the amino unit becomes more easily oxidized. The second oxidation peak is related to the electron losses from the side-chain TPA unit. According to the order of oxidation peaks of model compounds **M1**-**M3**, we propose a possible reaction sequence for the electrochemical oxidation of the series polyamides as shown in Scheme 3.

The HOMO (highest occupied molecular orbital) energy levels of the investigated polyamides were calculated from the oxidation onset potentials (E_{onset}) and by comparison with ferrocene (4.8 eV). These data together with absorption spectra were then used to obtain the LUMO (lowest unoccupied molecular orbital) energy levels (Table 1). According to the HOMO and LUMO energy levels obtained, the polyamides in this study appear to be appropriate as hole injection and transport materials.

Table 2. Redox Potentials and Energy Levels of Polyamides

Polymer code	Thin film absorption (nm)		Oxidation potential (V)[a]						E_g (eV)[b]	Energy level (eV)			
			E_{onset}		$E_{1/2}^{ox1}$		$E_{1/2}^{ox2}$			HOMO[c]		LUMO[d]	
	λ_{max}^{abs}	λ_{onset}^{abs}	CV	DPV	CV	DPV	CV	DPV		CV	DPV	CV	DPV
8a	305	458	0.60	0.61	0.81	0.79	0.94	0.96	2.70	5.17	5.15	2.47	2.45
8b	309	411	0.61	0.61	0.82	0.82	0.94	0.97	3.02	5.18	5.18	2.16	2.16
8c	305	500	0.70	0.58	0.81	0.80	0.96	0.95	2.48	5.17	5.16	2.69	2.68
8d	303	409	0.63	0.62	0.82	0.80	0.95	0.96	3.03	5.18	5.16	2.15	2.13

[a] From cyclic votammograms versus Ag/AgCl in CH_3CN. $E_{1/2}$: Average potential of the redox couple peaks. [b] The data were calculated from polymer films by the equation: $E_g = 1240/\lambda_{onset}$ (energy gap between HOMO and LUMO). [c] The HOMO energy levels were calculated from cyclic voltammetry and were referenced to ferrocene (4.8 eV). [d] LUMO = HOMO − E_g.

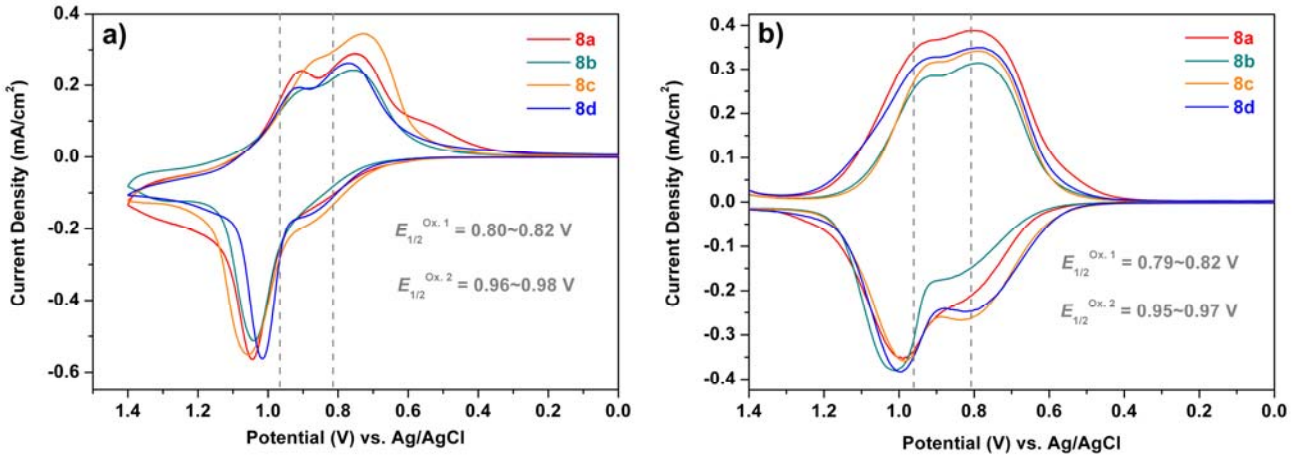

Figure 3. (a) Cyclic voltammograms and (b) differential pulse voltammograms of the cast films of polyamides **8a-8d** on the ITO-coated glass slide in 0.1 M Bu_4NClO_4/CH_3CN at scan rate of 50 mV/s.

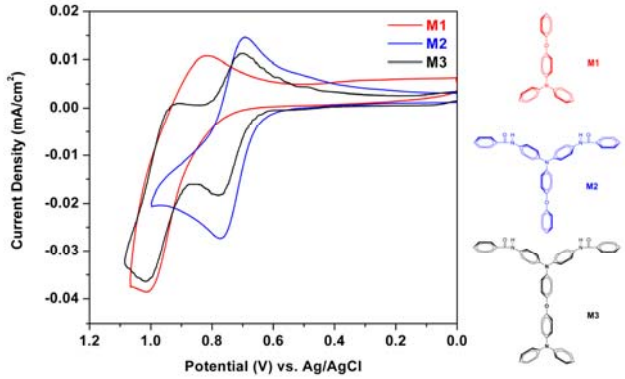

Figure 4. Cyclic voltammetric diagrams of model compounds **M1**, **M2** and **M3** in 0.1 M Bu_4NClO_4/CH_3CN solution at a scan rate of 50 mV/s.

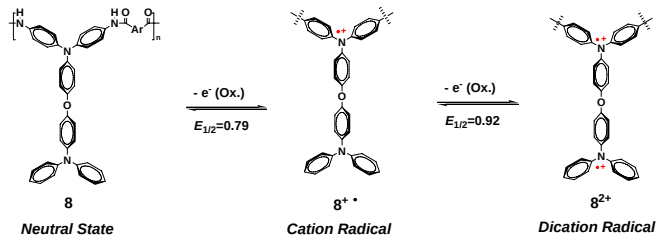

Scheme 3. Anodic oxidation pathways of the polyamides.

7. Spectroelectrochemical and Electrochromic Properties

Spectroelectrochemical measurements were performed on films of polymers drop-coated onto ITO-coated glass slides immerged in electrolyte solution. The electrode preparations and solution conditions were identical to those used in the CV experiments. Figure 5 presents the UV-vis-NIR absorption spectra of polyamide

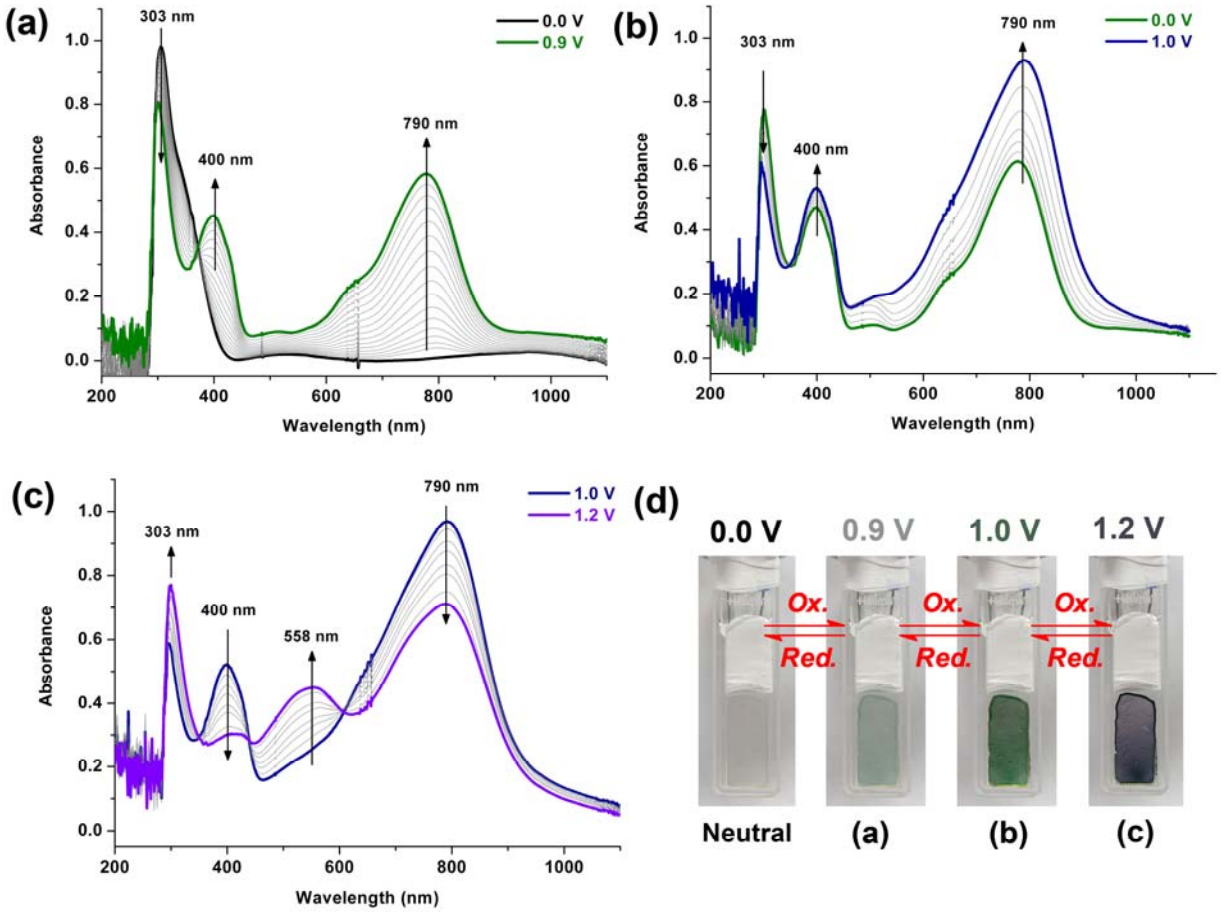

Figure 5. Spectroelectrochemistry of the polyamide **8d** thin film on the ITO-coated glass substrate in 0.1 M Bu_4NClO_4/CH_3CN at (a) 0.9 V, (b) 1.0 V, and (c) 1.1 V. The photos (d) show the color change of the film on an ITO electrode at indicated potentials.

8d film at various applied potentials. In the neutral form, polyamide **8d** exhibited strong absorptions at 303 nm, characteristic for the TPA moiety, but it was almost transparent in the visible region. When the applied voltage was stepped from 0 to 0.9~1.0 V, the intensity of the absorption peak around 303 nm decreased gradually, and new peaks at 400 and 790 nm gradually increased in intensity (Figure 5a and 5b). We attribute these spectral changes to the formation of a stable cation radical of the main-chain TPA moiety. Upon further oxidation at applied voltages to 1.2V, corresponding to the second step oxidation, the peaks of characteristic absorbance of the radical cation decreased gradually and one new band grew up at 558 nm (Figure 5c). The new spectrum was assigned as a dication of polyamide **8d**. The observed electronic absorption changes in the film of **8d** at various potentials are fully reversible and are associated with strong color changes; indeed, they even can be seen readily by the naked eye. From the photos shown in Figure 5d, it can be seen that the film changed from a transmissive neutral state (nearly colorless) to a highly absorbing semi-oxidized state (light green, green) and a fully oxidized state (purple).

7. Conclusions

A series of novel electroactive aromatic polyamides having $O(TPA)_2$ segments were readily prepared from the newly synthesized aromatic diamine monomer **6** with various aromatic dicarboxylic acids via the phosphorylation polyamidation reaction. Because of the introduction of three-dimensional triphenylamine units both in the main chain and in the side chain, all the polymers had good solubility in many polar aprotic solvents and exhibited excellent film-forming ability. In addition to moderately high T_g values and good thermal stability, all the obtained polyamides revealed good electrochemical and electrochromic stability along with multi-electrochromic behavior (highly transmissive-to-green and then to-purple switching). Such prominent features make these processable polymers amenable for optoelectronic applications such as OLEDs and electrochromic devices.

References

1 Monk, P. M. S.; Mortimer, R. J.; Rosseinsky, D. R. *Electrochromism and Electrochromic Devices*, Cambridge University Press, Cambridge, UK, 2007.

2 Beaujuge, P. M.; Reynolds, J. R. *Chem. Rev*. **2010**, *110*, 268.

3 (a) Balan, A.; Baran, D.; Gunbas, G.; Durmus, A.; Ozyurt, F.; Toppare, L. *Chem. Commun.* **2009**, 6768; (b) Invernale, M. A.; Ding, Y.; Mamangun, D. M. D.; Yavus, M. S.; Sotzing, G. A. *Adv. Mater.* **2010**, *22*, 1379; (c) Icli, M.; Pamuk, M.; Algi, F.; Onal, A. M.; Cihaner, A. *Org. Electron.* **2010**, *11*, 1255.

4 Shirota, Y.; Kageyama, H. *Chem. Rev.* **2007**, *107*, 953.

5 (a) Beaupre, S.; Breton, A-C.; Dumas, J.; Leclerc, M. *Chem. Mater.* **2009**, *21*, 1504; (b) Natera, J.; Otero, L.; D'Eramo, F.; Sereno, L.; Fungo, F.; Wang, N.-S.; Tsai, Y.-M.; Wong, K.-T. *Macromolecules* **2009**, *42*, 626.

6 (a) Cheng, S.-H.; Hsiao, S.-H.; Su, T.-H.; Liou, G.-S. *Macromolecules* **2005**, *38*, 307; (b) Hsiao, S.-H.; Chang, Y.-M.; Chen, H.-W.; Liou, G.-S. *J. Polym. Sci., Part A: Polym. Chem.* **2006**, *44*, 4579; (c) Chang, C.-W.; Liou, G.-S.; Hsiao, S.-H. *J. Mater. Chem.* **2007**, *17*, 1007; (d) Hsiao, S.-H.; Liou, G.-S.; Kung, Y.-C.; Yen, H.-J. *Macromolecules* **2008**, *41*, 2800; (e) Hsiao, S.-H.; Liou, G.-S.; Wang, H.-M. *J. Polym. Sci., Part A: Polym. Chem.* **2009**, *47*, 2330; (f) Wang, H.-M.; Hsiao, S.-H.; Liou, G.-S.; Sun, C.-H. *J. Polym. Sci. Part A: Polym. Chem*. **2010**, *48*, 4775; (g) Kung, Y.-C; Hsiao, S.-H. *J. Mater. Chem.* **2010**, *20*, 5481.

7 Yamazaki, N.; Matsumoto M; Higashi, F. *J. Polym. Sci. Polym. Chem. Ed.* **1975**, *13*, 1375.